Estimating greenhouse gas emissions and absorption in rice biomass with multi-temporal remote sensing and machine learning

Nguyen Mai Linh[1], Do Thi Nhung[2], Dang Do Lam Phuong[2], Nguyen Thi Thu Hang[1], Pham Van Manh[1*]

[1]*VNU University of Science, Vietnam National University, Hanoi*

[2]*University of Science and Technology of Hanoi*

Ước tính lượng phát thải và hấp thụ khí nhà kính trong sinh khối lúa bằng viễn thám đa thời gian và học máy

Nguyễn Mai Linh[1], Đỗ Thị Nhung[2], Đặng Đỗ Lâm Phương[2], Nguyễn Thị Thu Hằng[1], Phạm Văn Mạnh[1*]

[1]*Trường Đại học Khoa học Tự nhiên, Đại học Quốc gia Hà Nội*

[2]*Trường Đại học Khoa học và Công nghệ Hà Nội*

**Corresponding author: manh10101984@gmail.com*

https://doi.org/10.55250/jo.vnuf.11.2.2026.062-071

Article info:
Received: 13/04/2026
Revised: 25/05/2026
Accepted: 23/06/2026

Keywords:
Machine learning models, paddy rice, Red River Delta, Sentinel-1A SAR, time-series data.

ABSTRACT

Reducing greenhouse gas (GHG) emissions while optimizing rice cultivation is a major challenge for agricultural countries such as Vietnam, which aims to achieve net-zero emissions and strengthen climate change mitigation by 2050. Although rice production is essential for food security, it is also a primary source of CH_4, N_2O, and CO_2 emissions. Developing and evaluating technical measures and management strategies is therefore necessary to reduce emissions without compromising productivity. This study uses an integrated model that combines multi-temporal Sentinel-1A SAR data with machine learning algorithms to estimate rice biomass carbon emissions and uptake in Hà Nội, Hưng Yên, and Ninh Bình provinces in the Red River Delta. Results from the Winter–Spring and Summer–Autumn cropping seasons indicate that total greenhouse gas emissions (CO_2, N_2O, CH_4) reached approximately 122 thousand tons, while total carbon uptake was estimated at about 354 thousand tons, resulting in a net carbon accumulation of roughly 232 thousand tons. These findings demonstrate that while rice cultivation emits substantial GHGs, rice biomass can sequester significant amounts of carbon. The study provides quantitative evidence to support sustainable emission-reduction policies in rice production. More broadly, integrating remote sensing and machine learning methods offers an effective approach for monitoring carbon dynamics and supporting cultivation practices and policies that balance environmental sustainability with food security.

Từ khóa:
Dữ liệu đa thời gian, Đồng bằng sông Hồng, mô hình học máy, lúa gạo, Sentinel-1A SAR.

TÓM TẮT

Giảm phát thải khí nhà kính (GHG) và tối ưu hóa canh tác lúa là những thách thức lớn đối với các quốc gia nông nghiệp như Việt Nam, nơi đặt mục tiêu đạt phát thải ròng bằng "0" và giảm tác động của biến đổi khí hậu vào năm 2050. Sản xuất lúa gạo rất quan trọng đối với an ninh lương thực, nhưng cũng là nguồn phát thải chính của CH_4, N_2O và CO_2. Vì vậy, cần phát triển và đánh giá các biện pháp kỹ thuật cũng như chiến lược quản lý nhằm giảm phát thải mà không làm giảm năng suất. Nghiên cứu này sử dụng mô hình tích hợp, kết hợp dữ liệu SAR đa thời gian từ Sentinel-1A với các thuật toán học máy để ước tính lượng phát thải và hấp thụ carbon từ sinh khối lúa tại các tỉnh Hà Nội, Hưng Yên và Ninh Bình thuộc Đồng bằng sông Hồng. Kết quả từ các vụ Đông Xuân và Hè Thu cho thấy tổng lượng phát thải khí nhà kính (CO_2, N_2O, CH_4) khoảng 122 nghìn tấn, trong khi tổng lượng hấp thụ carbon ước tính khoảng 354 nghìn tấn, dẫn đến tích lũy carbon ròng khoảng 232 nghìn tấn. Kết quả này cho thấy trồng lúa phát thải khí nhà kính đáng kể, nhưng sinh khối lúa cũng hấp thụ một lượng carbon lớn. Nghiên cứu cung cấp bằng chứng định lượng để hỗ trợ các chính sách giảm phát thải bền vững trong sản xuất lúa gạo. Ngoài ra, việc kết hợp các phương pháp viễn thám và học máy mang lại một cách tiếp cận hiệu quả để giám sát động thái carbon, hỗ trợ các hoạt động canh tác, cũng như xây dựng các chính sách cân bằng giữa bảo vệ môi trường và đảm bảo an ninh lương thực.

1. INTRODUCTION

Rice is a staple food for over 4 billion people worldwide and is widely cultivated across tropical Asia [1]. Among major rice-producing countries, Vietnam is a leading exporter, with intensive rice cultivation concentrated in deltas such as the Mekong and Red River deltas [2]. Increasing rice production is challenging due to

limited arable land, population growth, and urbanization [3]. During rice cultivation, paddy fields account for about 25% of global freshwater used for irrigation [4]. At the same time, rice-growing activities are major sources of CH_4, CO_2, and N_2O emissions, which contribute to the greenhouse effect [5]. Large-scale mapping and estimation of rice field distribution are therefore essential for production planning, water management, climate adaptation, and policy decisions. However, field surveys for large-scale rice mapping require significant time, labor, and financial resources. Remote sensing using optical and radar (SAR) sensors enables large-scale data collection for biomass estimation and rice field monitoring [6]. Most previous studies have used optical sensors with different spatial resolutions, such as MODIS, Landsat, and Sentinel-2, to monitor and estimate rice yield [7]. However, frequent cloud cover during the growing season often limits optical sensors' effectiveness. By contrast, SAR systems produce high-quality imagery in all weather conditions, making them more reliable for monitoring crop growth and biomass [8].

Above-ground biomass can be estimated using both destructive and non-destructive methods [9]. Although highly accurate, field measurement methods are impractical for large-scale applications since they are time-consuming, labor-intensive, and costly because they require harvesting and processing samples to estimate both fresh and dry biomass [10]. In addition, the timely estimation of rice biomass is essential since biomass varies by season and environmental conditions [11].

Consequently, remote sensing provides an efficient approach to estimating rice biomass at large scales without direct contact. Recent advances in machine learning (ML) and deep learning (DL) have improved rice field mapping and crop monitoring using remote sensing data. Conventional ML algorithms, including artificial neural networks (ANN), Gaussian process regression (GPR), Decision Trees, K-Nearest Neighbors (K-NN), support vector machines (SVM), random forests (RF), Cubist, naive Bayes, and boosting (XGBoost, AdaBoost, Gradient), have demonstrated their effectiveness in processing remotely sensed data. More recently, deep convolutional neural networks (DCNNs) have become prominent for directly extracting features from raw imagery, resulting in improved classification accuracy [12]. Meanwhile, the adaptive neuro-fuzzy Inference system (ANFIS) has shown potential for rice biomass estimation by modeling nonlinear relationships between SAR backscatter and plant characteristics [13]. However, integrating DCNN-based rice field extraction with ANFIS-based biomass estimation using multi-temporal SAR data remains limited, particularly across different growing seasons.

This study, therefore, aims to fill these gaps by: (i) assessing the feasibility of a DCNN model for extracting rice fields from multi-temporal SAR imagery and (ii) estimating rice biomass using a multivariate linear regression-based ANFIS model. The analysis uses multi-temporal Sentinel-1A SAR data from the Winter-Spring and Summer-Autumn seasons, explicitly capturing seasonal changes in crop growth. The approach is particularly suitable for regions with frequent cloud cover and increasingly unstable weather conditions under current climate variability. The results are expected to support more consistent large-scale rice monitoring and provide additional information for agricultural management in the Red River Delta (RRD).

2. RESEARCH METHODS

2.1. Study area

The study area includes three provinces in the Red River Delta (RRD): Hà Nội, Hưng Yên, and Ninh Bình (Figure 1). The RRD is a major agricultural region, characterized by fertile alluvial soils and a dense river network that supports intensive rice cultivation. Spanning approximately 10,000 km² and supporting a population of 16.6 million, it ranks among the most densely populated regions in Vietnam, with more than 1,000 people per square kilometer [14]. Hà Nội serves as the national capital and the political, economic, and cultural center, while Hưng Yên and Ninh Bình are established cultural centers of the Northern Delta and important contributors to the wet-rice civilization. These provinces are essential to regional rice production because of their extensive cultivated areas, high yields, and strong domestic demand. Rice cultivation

primarily occurs in two seasons: Winter-Spring (January-May), which generally covers a larger area and yields higher production, and Summer-Autumn (June-November).

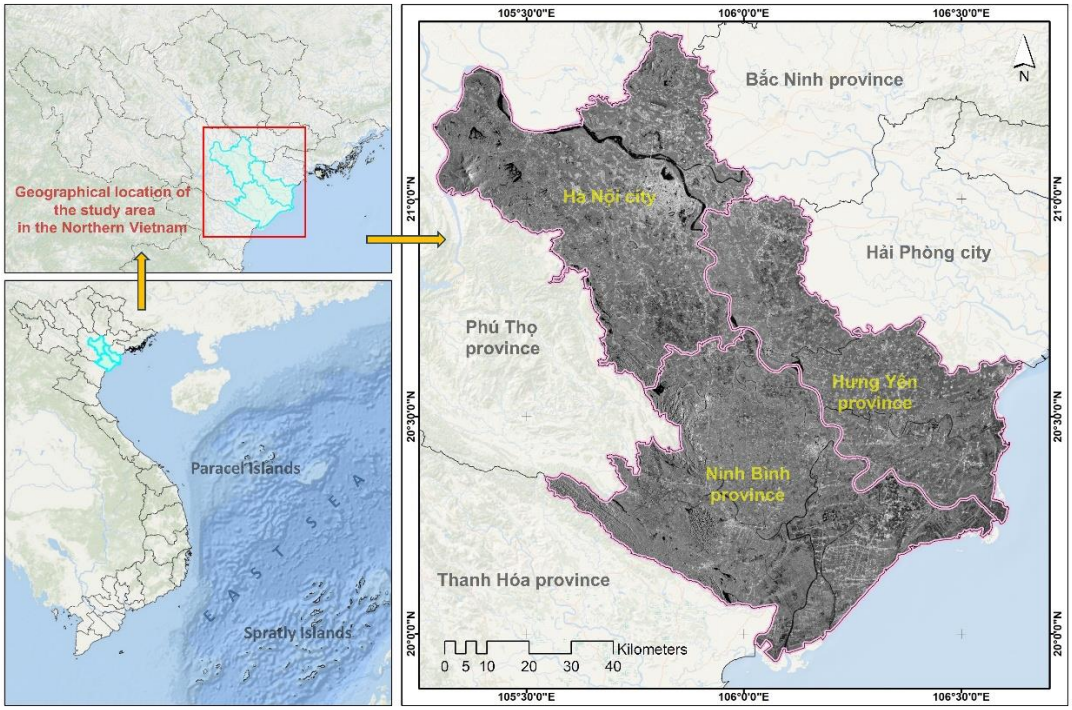


Figure 1. The study area and the locations of sample plots (Sentinel-1A satellite images, 2025)

2.2. Methods

2.2.1. In-situ biomass and Sentinel-1A SAR data processing

We measured rice biomass over two cropping seasons in 2025 using 115 randomly selected 10×10 meter plots. We divided the collected data (including plant counts, plant height, the number of plants per hill, and the number of hills per plot) into training and testing sets at a 70:30 ratio. We recorded sowing and harvesting dates to monitor growth stages and identify the optimal timing for estimating biomass using Sentinel-1A SAR. Radar data captures both surface and volume scattering from rice plants. Incident waves penetrate the canopy, interact with plant components, and generate backscatter signals that reflect vegetation characteristics, thereby enabling biomass estimation (Figure 2). The primary scattering mechanisms are: (i) canopy scattering, (ii) stem–soil interface scattering, (iii) stem scattering, (iv) multiple stem–soil scattering, (v) ground attenuation, and (vi) soil surface scattering.

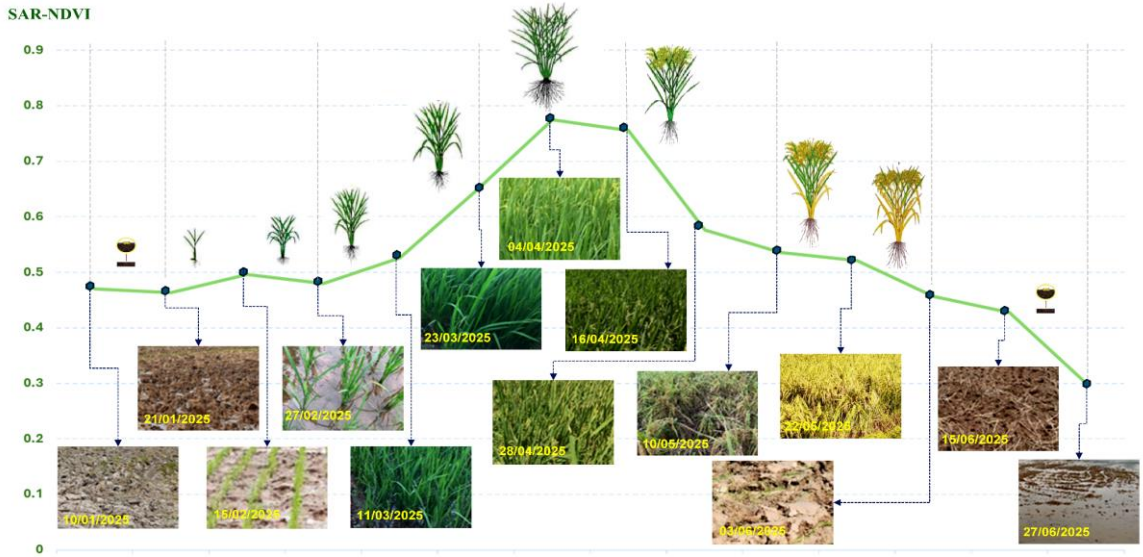


Figure 2. Radar backscatter of rice based on SAR-NDVI=sqrt{(VH–VV)/(VH+VV)}

29 Sentinel-1A Level-1 GRD scenes in VH and VV polarizations, collected every 12 days, to monitor rice fields across three provinces during the main cropping seasons. This dataset covers January to October and includes both major rice-growing periods. Preprocessing in SNAP with the Sentinel-1 Toolbox comprised normalization and noise reduction, speckle filtering using an adaptive Frost filter (7×7 window), terrain correction with a 10-m digital elevation model to minimize topographic distortions, and conversion of digital numbers to calibrated backscatter coefficients (σ0) to ensure radiometric consistency. Some previous studies have derived rice-sensitive indices from Sentinel-1A, which are affected by canopy structure and water conditions for crop monitoring and biomass estimation [6,15]. Drawing on this body of research, the present study selected indices including VH, VV, (VH–VV), (VH+VV), (VV–VH), (VH×VV), (VH+VV)/2, sqrt(VV–VH), sqrt(VV×VH), sqrt(VV/VH), and sqrt((VH–VV)/(VH+VV)), to build the rice biomass estimation model (Figure 3).

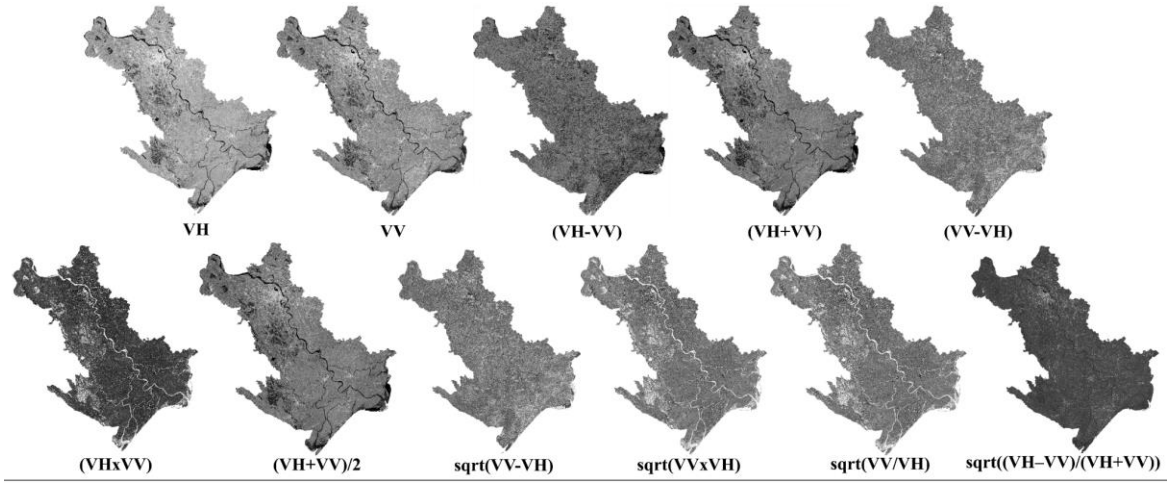


Figure 3. The indices were calculated from Sentinel-1A SAR imagery

2.2.2. Convolutional Neural Network for paddy rice mask

Convolutional neural networks (CNNs) represent input images as pixel matrices, enabling them to capture spatial relationships among neighboring pixels [16]. Rice field extraction using DCNNs generally involves inputting image data, applying convolutional and pooling layers, flattening the resulting feature maps, and processing them through fully connected and output classification layers (Figure 4). The CNN model utilized in this study was implemented in Python and sourced as open-source software from the GitHub repository vzhou842/cnn-from-scratch. The convolutional layer extracts features from satellite images using filters, and the rectified linear unit (ReLU) activation function accelerates training by setting negative values to zero (Eq.1). The pooling layer reduces spatial dimensions and the number of parameters through Max Pooling (Eq.2). Following multiple convolutional and pooling operations, the feature maps are flattened and processed by fully connected layers, which utilize the softmax activation function for classification (Eq.3).

$$y(i) = \sum_{j=1}^{F} x(i+j-1)w(j)\ ;\ \text{mand ReLU(x)=max(0, x)} \quad \text{(Eq.1)}$$

$$y(i,j) = \max(y[i:i+f, j:j+f]) \quad \text{(Eq.2)}$$

$$soft\max(z_i) = e^{z_i} / \sum_{j=1}^{n} e_j \quad \text{(Eq.3)}$$

where;

y(i) denotes the i-th component of the feature map;

x represents the input data;

w is the kernel filter of length F;

j indicates the filter's sliding position;

f specifies the pooling window size;

zi is the output of the neuron in the fully connected layer;

n is the number of output classes.

The one-dimensional CNN (C1) extracts sequential patterns from Sentinel-1A SAR

backscatter using three convolutional layers, a flattening layer, and three fully connected layers. The multi-dimensional CNN (C2) captures spatial relationships and reduces heterogeneous noise through three convolutional layers, pooling, flattening, and normalization. Both models use ReLU activation and softmax for pixel-wise classification, generating binary rice masks (0 = non-rice, 1 = rice). Performance was evaluated using overall accuracy (OA) and cross-validation accuracy (CV), as described in Section 2.2.4.

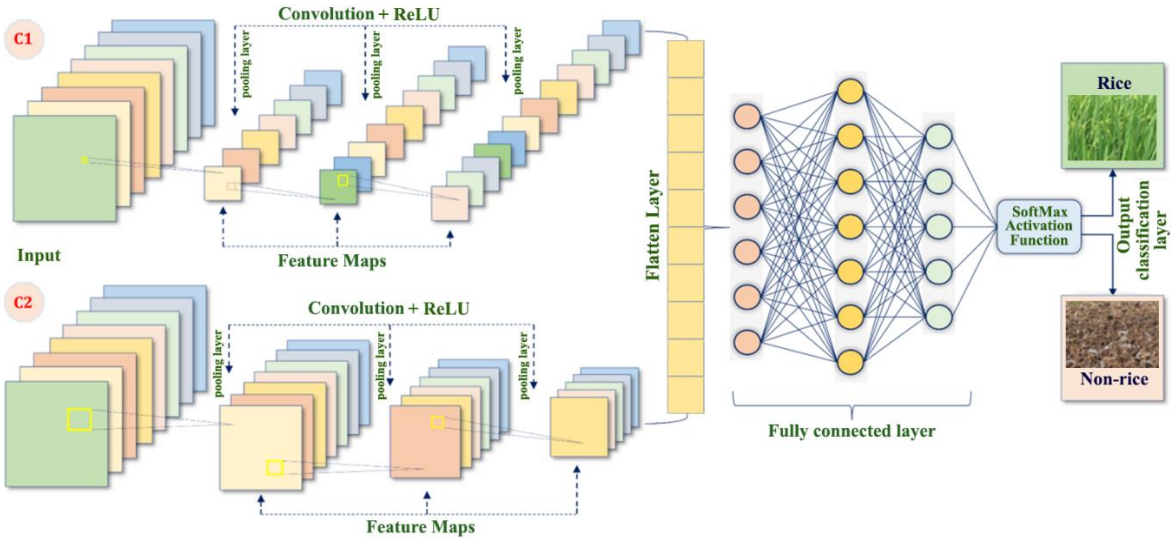


Figure 4. Structure of the DCNN deep learning model used in this study

2.2.3. Adaptive neuro-fuzzy inference system for rice biomass

The adaptive neuro-fuzzy inference system (ANFIS) is commonly utilized for multivariate regression problems. Its architecture combines fuzzy inference with neural network components and consists of five fixed layers, with the number of hidden nodes corresponding to the five fuzzy system layers. In this research, the open-source Python ANFIS implementation is available from the GitHub repository twmeggs/anfis. ANFIS rules are structured in an "if-then" format, linking antecedents to outcomes as shown in (Eq.4).

$$\textit{If } Z_k \text{ is } A_{kj}, \textit{ then } y^{(j)}=\theta_{j0}+\sum_{k=1}^{p}\theta_{jk}Z_k\theta_{jk} \quad \text{(Eq.4)}$$

where, Z_k is A_{kj} as the premise section, and $y^{(j)}=\theta_{j0}+\sum_{k=1}^{p}\theta_{jk}Z_k\theta_{jk}$ as the consequent section; θ_{j0}, θ_{jk} are linear parameters; A_{kj} are nonlinear parameters; j=1,2…m; k=1,2…*p*; and can be estimated through several steps as described in the following five layers:

Layer-1: This layer processes training data with 12 predictor variables (see Figure 5). Clustering determines the optimal number of clusters, while each adaptive node applies a parametric activation function to calculate input membership degrees, as defined in (Eq.5).

$$\mu_{A_{kj}}(Z_k)=\exp\left(-\frac{1}{2}\left(\frac{Z_k-c_{jk}}{a_{jk}}\right)^2\right), j=1,2...m; k=1,2...p \quad \text{(Eq.5)}$$

where, c_{jk} is the location parameter, and a_{jk} is the scaling parameter. These are the premise parameters and were fed into the next layer.

Layer-2: Every node in the second layer is a fixed node, and its output is the product of the incoming signal, the membership function, and the following (Eq.6).

$$W_j=\prod_{k=1}^{p}\mu_{A_{kj}}, j=1,2...m \quad \text{(Eq.6)}$$

Layer-3: Every node in the third layer is a fixed node, which computes the ratio of firing strength, and weights are normalized in this step by (Eq.7).

$$\overline{W}_j=\frac{W_j}{\sum_{j=1}^{m}W_j} \quad \text{(Eq.7)}$$

Layer-4: Every node in the fourth layer is an adaptive layer and takes the sum of linear functions multiplied by normalized weights in the previous step. The output of each node is calculated as follows (Eq.8).

$$\overline{W}_j y^{(j)}=\overline{W}_j\left(\theta_{j1}Z_1+\theta_{j2}Z_2+...+\theta_{jp}Z_p+\theta_{j0}\right) \quad \text{(Eq.8)}$$

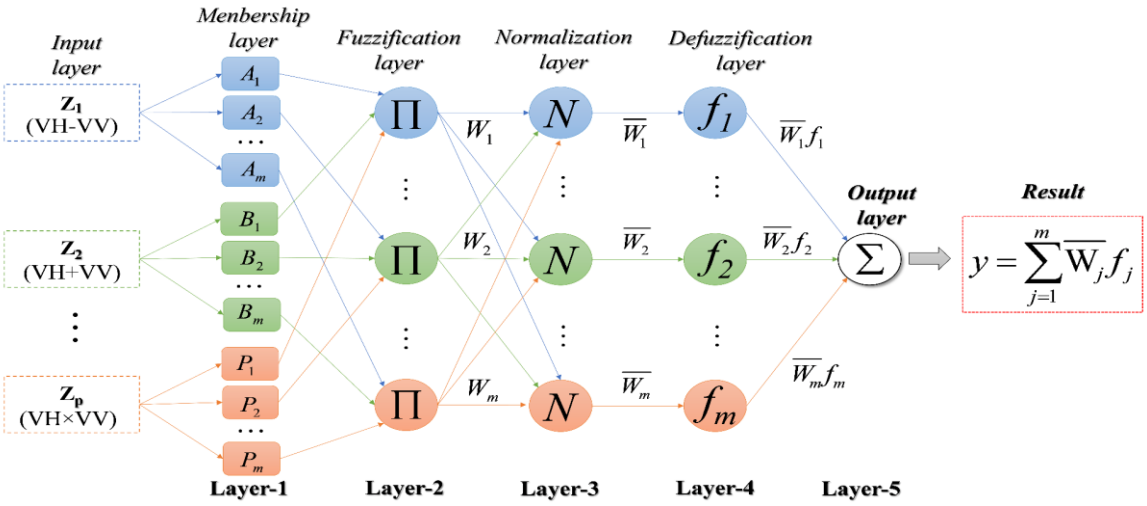


Figure 5. The architecture of the adaptive neuro-fuzzy inference system (ANFIS) model

Layer-5: Every node in the fifth layer is a fixed node that sums all incoming signals. The output of the whole network can be calculated by (Eq.9).

$$y = \sum_{j=1}^{m} \overline{W}_j \left(\theta_{j1} Z_1 + \theta_{j2} Z_2 + \ldots + \theta_{jp} Z_p + \theta_{j0} \right) \quad \text{(Eq.9)}$$

When the ANFIS model is given as (Eq.10), then the estimation of the consequent parameters of ANFIS (θ_{jk} , j=1,2…m; and k=1,2…p) can use the adaptive filtering algorithm, Recursive Least Squares, to reduce the mean squared error (RMSE).

After estimating the consequent parameters, the premise parameters can be updated by backpropagating errors. Optimal quality is achieved by minimizing the ANFIS error function. To evaluate the ANFIS model's accuracy, the study uses the coefficient of determination (R^2) and root mean square error (RMSE), as presented in Section 2.2.4.

$$\hat{\theta}_{11}(\overline{w}_1 Z_{t-1}) + \hat{\theta}_{12}(\overline{w}_1 Z_{t-2}) + \ldots + \hat{\theta}_{1p}(\overline{w}_1 Z_{t-p}) + \hat{\theta}_{10}\overline{w}_1 + \hat{\theta}_{21}(\overline{w}_2 Z_{t-1}) + \hat{\theta}_{22}(\overline{w}_2 Z_{t-2}) + \ldots + \hat{\theta}_{2p}(\overline{w}_2 Z_{t-p}) + \hat{\theta}_{20}\overline{w}_2 + \ldots + \hat{\theta}_{m1}(\overline{w}_m Z_{t-1}) + \hat{\theta}_{m2}(\overline{w}_m Z_{t-2}) + \ldots + \hat{\theta}_{mp}(\overline{w}_m Z_{t-p}) + \hat{\theta}_{m0}\overline{w}_m = Z_t \quad \text{(Eq.10)}$$

2.2.4. Accuracy assessment of DCNN and ANFIS models in rice biomass estimation

The authors evaluated the accuracy of the DCNN and ANFIS models in rice field extraction using overall accuracy (OA) and cross-validation accuracy (CV). They assessed the rice biomass estimation model's reliability with the coefficient of determination (R^2) and root mean square error (RMSE).

$$OA = \frac{TP+TN}{TN+TP+FN+FP} \quad \text{(Eq.11)}$$

$$CV = \frac{\frac{2\times TP}{(TP+FN)} \times \frac{TP}{(TP+FP)}}{\frac{TP}{(TP+FN)} + \frac{TP}{(TP+FP)}} \quad \text{(Eq.12)}$$

$$RMSE = \sqrt{\frac{1}{n}\sum_{i=1}^{n}(Y_i - X_i)^2} \quad \text{(Eq.13)}$$

$$R^2 = \frac{\sum_{i=1}^{n}[(Y_i-\bar{Y}_i)(X_i-\bar{X}_i)]}{\sqrt{\sum_{i=1}^{n}(Y_i-\bar{Y}_i)^2 \times \sqrt{\sum_{i=1}^{n}(X_i-\bar{X}_i)^2}}} \quad \text{(Eq.14)}$$

True Positive (TP) indicates correctly classified rice fields, whereas True Negative (TN) refers to correctly classified non-rice fields. False Positive (FP) denotes non-rice fields incorrectly classified as rice fields, and False Negative (FN) denotes rice fields incorrectly classified as non-rice fields. Variables and their mean values represent estimated data compared to field-measured data, with n denoting the sample size. Model performance was evaluated using the coefficient of determination (R^2), which ranges from 0 to 1, and the root mean square error (RMSE). An optimal model demonstrates a high R^2 and a low RMSE.

2.2.5. Integrated evaluation of greenhouse gas emissions from rice biomass

Quantifying greenhouse gas (GHG) emissions from rice biomass is essential to assess the climate impact of rice production. We consider emissions from both rice growth and biomass burning, focusing on the three main agricultural gases: CO_2, CH_4, and N_2O (Eq.15–17). The calculation also accounts for CO_2-equivalent absorption by rice biomass

(Eq.18). Carbon credits are valued based on the net CO_2 balance (Eq.19). To ensure accuracy and relevance, we verified all equations and parameters against published guidelines, reports, and previous studies. Total GHG emissions are calculated as follows:

$$CO_2 = CO_{2(fertilizer)} + CO_{2(burning)} = M \times EF_{CO_2} \times 44/12 + A \times Mb \times Cf \times EF_{CO_2} \quad \text{(Eq.15)}$$

$$CH_4 = CH_{4(rice\ growth)} + CH_{4(burning)} = EF_{CH_4} \times A \times t + A \times Mb \times Cf \times EF_{CH_4} \quad \text{(Eq.16)}$$

$$N_2O = N_2O_{(rice\ growth)} + N_2O_{(burning)} = N_{(input)} \times EF_{N_2O} \times \frac{44}{28} + A \times Mb \times Cf \times EF_{N_2O} \quad \text{(Eq.17)}$$

$$CO_2e = 0.08 \times (AGB_{rice} \times 3.67) \quad \text{(Eq.18)}$$

$$Carbon\ Credits = CO_2 absorption - CO_2 emission - CO_2 fertilizer - CO_2 burning \quad \text{(Eq.19)}$$

where;

M denotes nitrogen fertilizer applied per season (ton/season);

EF represents the emission factor specific to each gas and process;

A is the cultivated area (m² or ha);

Mb is dry biomass adjusted by a conversion factor (ton/area);

Cf is the combustion coefficient indicating the fraction of biomass burned;

t is the cultivation period (days);

N(input) is the nitrogen input used in N_2O emission calculations (ton/season).

3. RESULTS AND DISCUSSION

3.1. Machine learning models for estimating paddy rice masking and biomass prediction from multi-temporal remote sensing

The one-dimensional (C1) and multi-dimensional (C2) convolutional neural network classifiers in the DCNN model performed strongly, with overall accuracy (OA) and cross-validation (CV) above 0.85. For the Winter-Spring rice crop, OA was 0.89, and CV was 0.86. The Summer-Autumn rice crop achieved OA of 0.87 and CV of 0.85. Training and testing times for both classifiers were within acceptable limits [17]. We produced spatial distribution maps of rice fields for both crops (Figure 6). Field and collected data estimated the Winter-Spring rice cultivation area at 523,805 ha. The CIAT (Rice report for the Northern Midlands and Mountains and the Red River Delta, 2025) reported approximately 511,201 ha for the same crop in 2025. The area extracted from Sentinel-1A SAR imagery achieved a high accuracy of 95.77% compared to these statistics. The cultivated area for the Summer-Autumn rice crop was 513,102 ha, which is 10,703 ha less than the Winter-Spring crop.

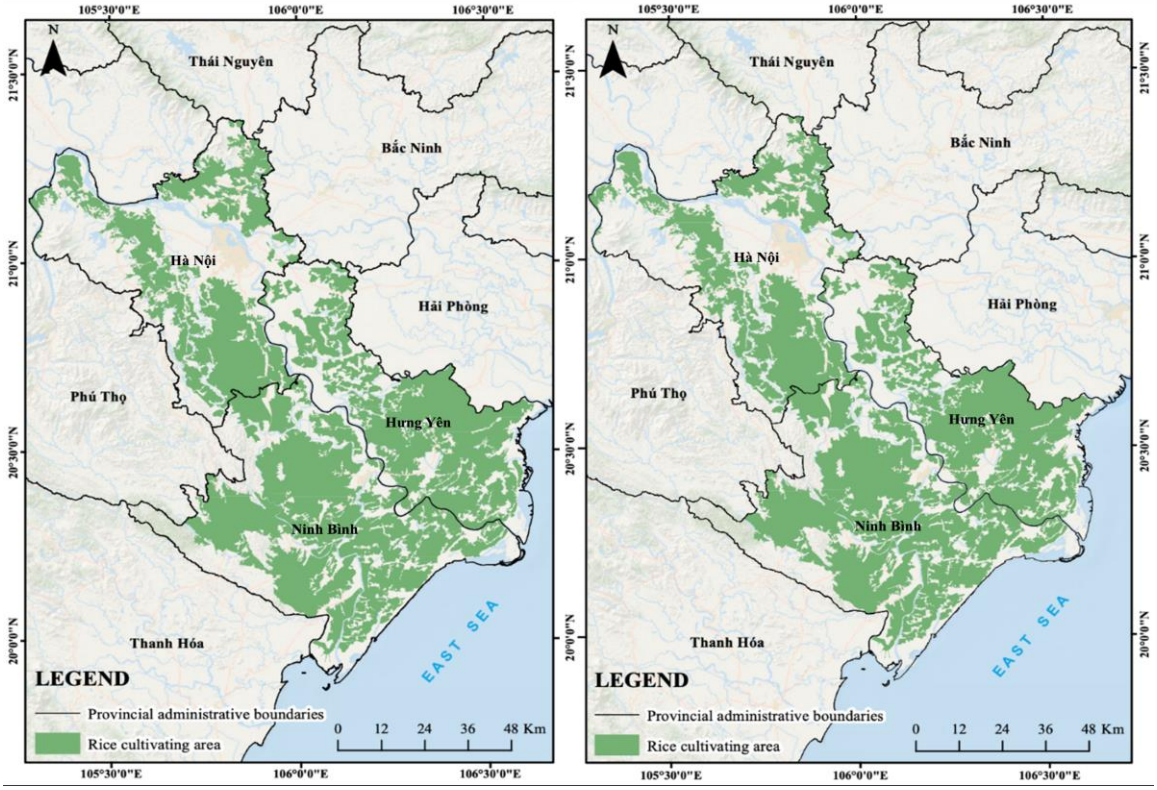


Figure 6. Spatial distribution of rice cultivation area for the Winter-Spring rice crop (left panel) and Summer-Autumn rice crop (right panel) in 2025

The authors used the rice biomass equation (Eq.20), derived from the ANFIS model, to generate two spatial maps of aboveground rice biomass. We validated these maps against field measurements, and they showed close agreement: for the Winter–Spring crops, R^2=0.80 with RMSE = 0.11 kg, and for the Summer–Autumn crops, R^2=0.78 with RMSE = 0.13 kg.

$$AGB_{rice} = 4.05 + 0.25 \times [\frac{(VH+VV)}{2}] + 0.2 \times \sqrt{\frac{(VV)}{(VH)}} + 5.5 \times \sqrt{\frac{(VH-VV)}{(VH+VV)}} \quad \text{(Eq.20)}$$

Spatial distribution maps of rice AGB at the heading stage in the study area were classified into five categories using the natural break algorithm (Figure 7), with refinement by agricultural experts: (i) AGB < 2.5 kg/m², (ii) 2.5–3.5 kg/m², (iii) 3.5–4.5 kg/m², (iv) 4.5–5.5 kg/m², and (v) > 5.5 kg/m². The 4.5–5.5 kg/m² category accounted for the largest proportion, approximately 70% in the Winter–Spring crops and 67% in the Summer–Autumn crops. Field measurements confirmed that Sentinel-1A data effectively monitor rice growth and estimate AGB.

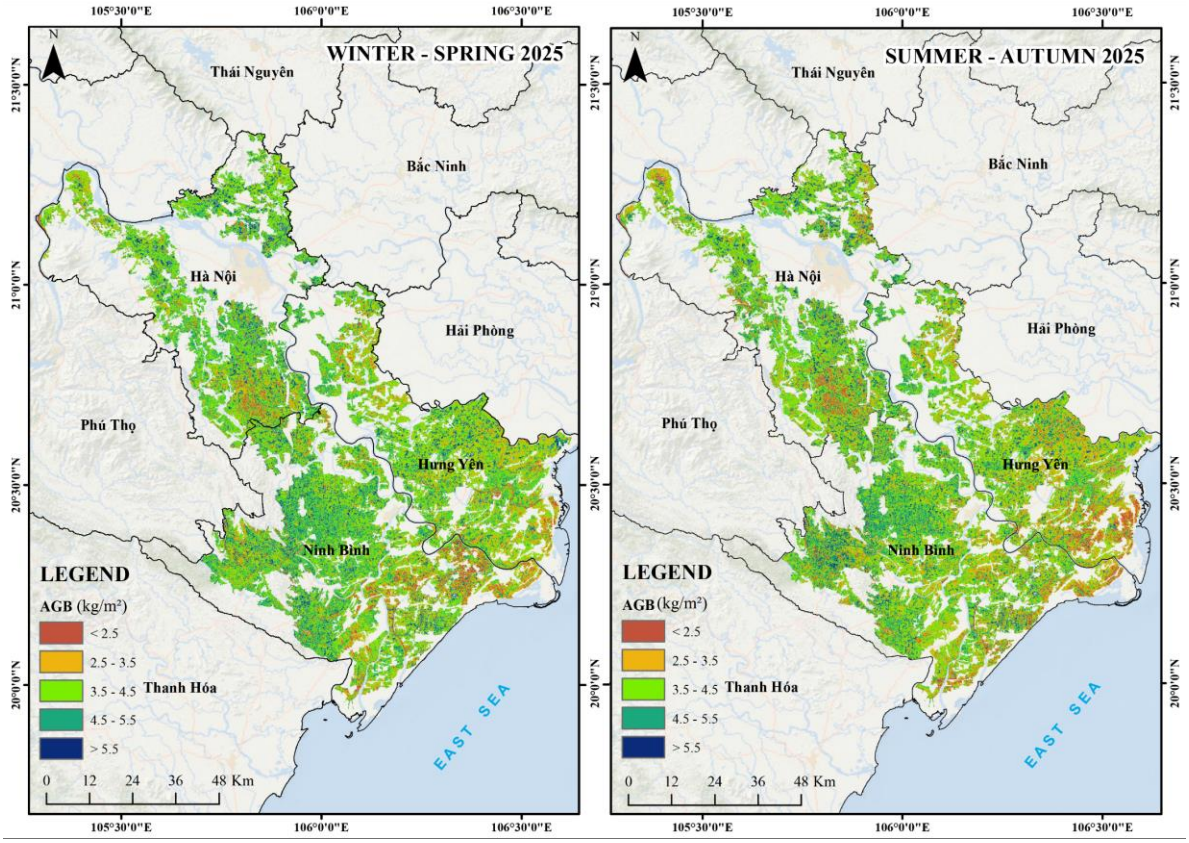


Figure 7. Spatial distribution of rice biomass in Winter-Spring and Summer-Autumn crops, 2025

The variables (VH+VV)/2, sqrt(VV/VH), and sqrt{(VH-VV)/(VH+VV)} were selected to identify the optimal model for estimating rice biomass. The ANFIS model applied to the Sentinel-1A SAR dataset performed best in estimating rice biomass during the reproductive stage [18]. This shows that downscaling biomass estimation to specific growth stages can yield more accurate estimates than season-long assessments. However, subdividing biomass estimates by growth stage may not suit operational scenarios that require timely data acquisition. It may be better suited for precision-agriculture applications where accuracy is prioritized.

3.2. Assessing greenhouse gas emissions and absorption from rice biomass

Greenhouse gas emissions (CO_2, CH_4, N_2O) from rice cultivation vary between the Winter–Spring and Summer–Autumn seasons and are unevenly distributed across the three provinces (Figure 8). Ninh Bình consistently reports the highest emissions for all gases, followed by Hà Nội, with Hưng Yên the lowest. CO_2 emissions

are approximately 43,000 tons in Winter–Spring and decrease slightly to 42,000 tons in Summer–Autumn. Although Ninh Bình leads in both seasons, provincial differences are minor, indicating that CO_2 emissions are primarily proportional to production scale. CH_4 emissions remain steady at about 18,000 tons in both seasons. N_2O emissions show little variation, declining from 473 tons in Winter–Spring to 472 tons in Summer–Autumn. Ninh Bình remains the largest contributor, while Hưng Yên consistently reports the lowest levels.

Rice CO_2 sequestration averaged 175,000 tons over two seasons. Ninh Bình led with 80,000 tons, followed by Hà Nội with 50,000 tons and Hưng Yên with 48,000 tons (Figure 9). Estimated 2025 carbon credits follow this pattern: Ninh Bình is projected to reach 129,000 credits, while Hà Nội and Hưng Yên are each expected to reach 70,000 credits. Although rice cultivation emits greenhouse gases, rice biomass sequesters substantial CO_2, partially offsetting these emissions. Unlocking economic value from carbon credits will require robust measurement, verification, and governance to ensure accuracy, transparency, and sustainability.

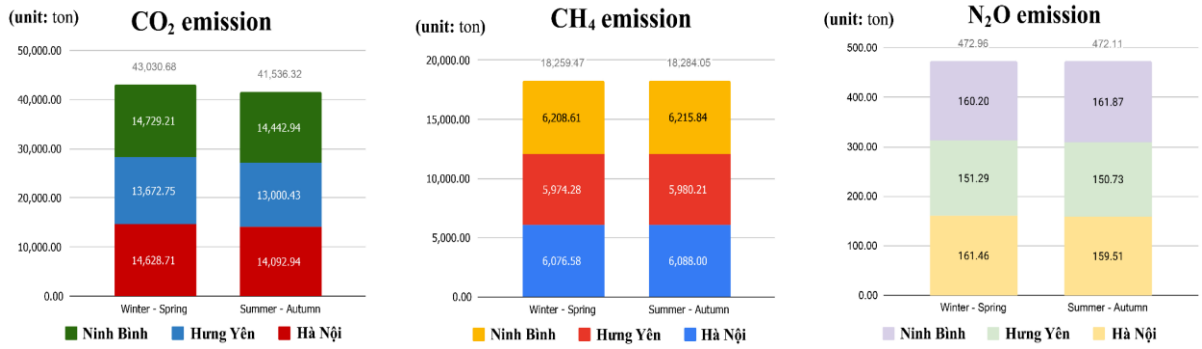


Figure 8. CO2, CH4, and N2O emissions of three provinces in two seasons in 2025

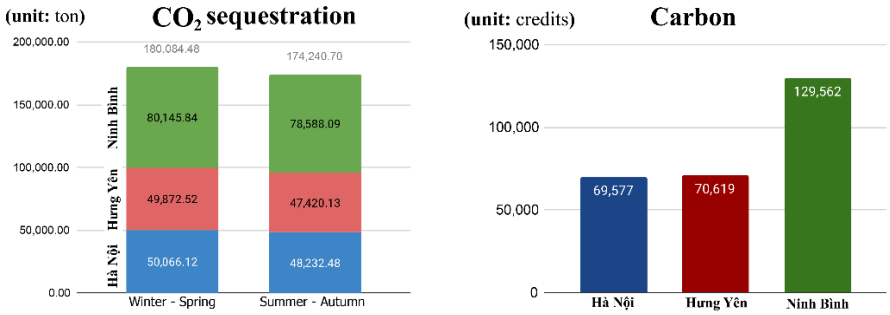


Figure 9. Carbon sequestration in two seasons and total Carbon credits of three provinces in 2025

4. CONCLUSION

This paper applies Sentinel-1A SAR data with machine learning (ANFIS) and deep learning (DCNN) methods for rice area classification and biomass estimation. Seasonal analysis shows that combining VH and VV polarizations using indices such as (VH+VV)/2, sqrt(VV/VH), and sqrt{(VH−VV)/(VH+VV)} increases accuracy compared with using each polarization separately. Biomass estimates are most accurate at the reproductive (heading) stage, suggesting that models tailored to specific growth stages—vegetative, reproductive (heading), and ripening—perform better. A stage-based modeling approach is recommended. Greenhouse gas balance analysis for 2025 indicates total emissions of about 122,000 tons, total CO_2 uptake of approximately 354,000 tons, and a net accumulation of roughly 232,000 tons over two seasons. These results suggest that rice cultivation could participate in the carbon credit market. To achieve this, further steps are required: expand observational samples, validate models at larger scales, improve input data quality, and establish robust measurement, reporting, and verification (MRV) systems to ensure accurate and sustainable carbon credits.

Acknowledgements

This work has been funded by the Vietnam National Foundation for Science and Technology Development (NAFOSTED) under grant number 105.08-2025.10. We thank the handling Editor and anonymous reviewers.

REFERENCES

[1]. Mishra, A. K., Pede, V. O., Arouna, A., Labarta, R., Andrade, R., Veettil, P. C., Bhandari, H., Laborte, A. G., Balie, J., & Bouman, B. (2022). Helping feed the world with rice innovations: CGIAR research adoption and socioeconomic impact on farmers. Global Food Security. 33: 100628. DOI: 10.1016/j.gfs.2022.100628

[2]. Tran, D. D., Park, E., Thu Van, C., Nguyen, T. D., Nguyen, A. H., Linh, T. C., Quyen, P. H., Tran, D. A., & Nguyen, H. Q. (2024). Advancing sustainable rice production in the Vietnamese Mekong Delta insights from ecological farming systems in An Giang province. Heliyon. 10(17): e37142. DOI: 10.1016/j.heliyon. 2024.e37142

[3]. Hashim, N., Ali, M. M., Mahadi, M. R., Abdullah, A. F., Wayayok, A., Mohd Kassim, M. S., & Jamaluddin, A. (2024). Smart Farming for Sustainable Rice Production: An Insight into Application, Challenge, and Future Prospect. Rice Science. 31(1): 47–61.
DOI: 10.1016/j.rsci.2023.08.004

[4]. Blango, M. M., Cooke, R. A. C., & Moiwo, J. P. (2019). Effect of soil and water management practices on crop productivity in tropical inland valley swamps. Agricultural Water Management. 222: 82-91.
DOI: 10.1016/j.agwat.2019.05.036

[5]. Chataut, G., Bhatta, B., Joshi, D., Subedi, K., & Kafle, K. (2023). Greenhouse gases emission from agricultural soil: A review. Journal of Agriculture and Food Research. 11: 100533.
DOI: 10.1016/j.jafr.2023.100533

[6]. Parag, M., Lottering, R., Peerbhay, K., Agjee, N., & Poona, N. (2024). The use of synthetic aperture radar technology for crop biomass monitoring: A systematic review. Remote Sensing Applications: Society and Environment. 33: 101107.
DOI: 10.1016/j.rsase.2023.101107

[7]. Kong, J., Ryu, Y., Dechant, B., Jeong, S., Kim, J., Lee, K., Ku, B., & Houborg, R. (2026). Uncovering the importance of spatiotemporal resolution in satellite-based rice yield estimation using a simple but effective proxy. Agricultural and Forest Meteorology. 376: 110892. DOI: 10.1016/j.agrformet.2025.110892

[8]. Vesterdal, M., Gislum, R., & Dalgaard, T. (2026). Current remote sensing applications for sustainable agricultural transitions and nature-based solutions. Journal of Environmental Management. 397: 128263. DOI: 10.1016/j.jenvman.2025.128263

[9]. Xu, T., Wang, F., Shi, Z., Xie, L., & Yao, X. (2023). Dynamic estimation of rice aboveground biomass based on spectral and spatial information extracted from hyperspectral remote sensing images at different combinations of growth stages. ISPRS Journal of Photogrammetry and Remote Sensing. 202: 169–183. DOI: 10.1016/j.isprsjprs.2023.05.021

[10]. Abudu, D., Chong, K., Bastin, L., & Röder, M. (2025). A meta-analysis of predictive accuracies and errors of biomass estimation models in Sub-Saharan Africa. Science of The Total Environment. 1001: 180455. DOI: 10.1016/j.scitotenv.2025.180455

[11]. Dela Torre, D. M. G., Gao, J., & Macinnis-Ng, C. (2021). Remote sensing-based estimation of rice yields using various models: A critical review. Geo-Spatial Information Science. 24(4): 580–603.
DOI: 10.1080/10095020.2021.1936656

[12]. Wardah, W., Khan, M. G. M., Sharma, A., & Rashid, M. A. (2019). Protein secondary structure prediction using neural networks and deep learning: A review. Computational Biology and Chemistry. 81: 1–8. DOI: 10.1016/j.compbiolchem.2019.107093

[13]. Kushwaha, A., Dave, R., Kumar, G., Saha, K., & Khan, A. (2022). Assessment of rice crop biophysical parameters using Sentinel-1 C-band SAR data. Advances in Spaceborne SAR Remote Sensing for Characterization of Natural and Manmade Features - Part 2. 70(12): 3833–3844. DOI: 10.1016/j.asr.2022.02.021

[14]. General Statistics Office of Vietnam (2025). Population – National Statistics Office of Vietnam.

[15]. Garcia, A. D. B., Islam, M. S., Prudente, V. H. R., Sanches, I. D., & Cheng, I. (2025). Irrigated rice-field mapping in Brazil using phenological stage information and optical and microwave remote sensing. Applied Computing and Geosciences. 25: 100223.
DOI: 10.1016/j.acags.2025.100223

[16]. Mohamed, E., Sirlantzis, K., & Howells, G. (2022). A review of visualization-as-explanation techniques for convolutional neural networks and their evaluation. Displays. 73: 102239. DOI: 10.1016/j.displa.2022.102239

[17]. Adegun, A., Viriri, S., & Tapamo, J.-R. (2024). Automated classification of remote sensing satellite images using deep learning-based vision transformer. Applied Intelligence. 54(24): 13018–13037.
DOI: 10.1007/s10489-024-05818-y

[18]. Agbaogun, B. K., Olu-Owolabi, B. I., Buddenbaum, H., & Fischer, K. (2023). Adaptive neuro-fuzzy inference system (ANFIS) and multiple linear regression (MLR) modelling of Cu, Cd, and Pb adsorption onto tropical soils. Environmental Science and Pollution Research. 30(11): 31085–31101. DOI: 10.1007/s11356-022-24296-8.